NO Answer from Face? Continuous Emotion Detection In EDA Signals

Huanghao Feng, *Member, IEEE,* and Mohammad Mahoor, *Fellow, IEEE,*

Abstract—

Index Terms—Affective Computing, Emotion Detection, Music, Human-Robot Interaction, Autism Spectrum Disorders.

1 Introduction

MUSIC, performed by instrument, is created to express emotions. However, learning how to play can be a different story, even to those who have talent in music. Facial expressions could be a reliable representation of emotions from individuals for most of the cases. However, it could be challenge for specific populations such as Autism Spectrum Disorders (ASDs), a grouping of disorders characterized by profound difficulties with social interaction, have demonstrated impairments in facial emotion recognition. Indeed, Kanner (1943) originally described autism as a 'disorder of affective contact', and the current DSM-IV-TR diagnostic criteria for ASDs include items related to deficits in identifying and processing emotions: "marked impairments in the use of multiple nonverbal behaviors, such as ...facial expression..." and "lack of social or emotional reciprocity" (APA 2000). There are three different perspectives dealing with affect in multimedia, namely, expressed emotions, felt emotions and expected emotions, Electrodemal activity (EDA) signals which is considered as a periphery

Feng
March 30, 2020

2 Background

2.1 Autism

Individuals with autism spectrum disorder experience verbal and nonverbal communication impairments, including motor control, emotional facial expressions, and eye gaze attention. Oftentimes, individuals with high-functioning autism have deficits in different areas, such as (1) language delay, (2) difficulty in having empathy with their peer and understanding others emotions (i.e. facial expressions recognition.), and more remarkably (3) joint attention (i.e. eye contact and eye gaze attention). Autism is a disorder that appears in infancy [**?**]. Although there is no single accepted intervention, treatment, or known cure for ASDs, these individual will have more successful treatment if ASD is diagnosed in early stages. At the first glance at the individual with autism, you may not notice anything odd, however after trying to talk to her/him, you will understand something is definitely not right [**?**]. S/He may not make eye contact with you and avoid your gaze and fidget, rock her/his body and bang her/his head against the wall [**?**]. In early 1990s, researchers in the University of California at San Diego aimed to find out the connections between autism and nervous system (i.e. mirror neurons). Mirror neuron [**?**] is a neuron that is activated either when a human acts an action or observes the same action performed by others. As these neurons are involved with the abilities such as empathy and perception of other individual's intentions or emotions, they came up with malfunctioning of mirror neuron in individuals with ASD [**?**]. There are several studies that focus on the neurological deficits of individuals with autism and studying on their brain activities. Figure 2-1 demonstrates the areas in the brain that causes the reduce mirror neuron activities in individuals with autism.

Individuals with autism might also have several other unusual social developmental behaviors that may appear in infancy or childhood. For instance children with autism show less attention to social stimuli (e.g. facial expressions, joint attention), and respond less when calling their names. Compared with typically developing children, older children or adults with autism can read facial expressions less effectively and recognize emotions behind specific facial expressions or the tone of voice with difficulties [**?**]. In contrast to TD individuals, children with autism (i.e. high-functioning, Asperger syndrome) may be overwhelmed with social signals such as facial behaviors and expression and complexity of them and they suffer from interacting with other individuals, therefore they would prefer to be alone. That is why it would be difficult for individuals with autism to maintain social interaction with others [**?**].

In order to diagnose and asses the aspects and score the social skill level of an individual with autism, several protocols are available. One of the commercially available protocols is called Autism Diagnostic Observation Schedule (ADOS) [**?**] that consists of four modules and several structured tasks that are used to measure the social interaction levels of the subject and examiner. We are

- *M. Shell was with the Department of Electrical and Computer Engineering, Georgia Institute of Technology, Atlanta, GA, 30332. E-mail: see http://mohammadmahoor.com/*
- *J. Doe and J. Doe are with Anonymous University.*

Manuscript created Feb 1, 2020; revised March 26, 2020.

inspired by ADOS in designing our intervention protocols later described in Chapter 4. Hence, we briefly review ADOS in the next section.

2.2 Human-Robot Interaction (HRI)

3 Experiment Setup and Data Collection

3.1 Xylo-Bot: An Interactive Music Teaching System

3.2 Video-Audio Annotation

4 Methods

"If you want to find the secrets of the universe, think in terms of energy, frequency and vibration."
–Nikola Tesla

4.1 EDA Signals

4.2 Complex-Morlet (C-Morlet) Wavelet Transform

4.2.1 Continuous Wavelet Transform

The EDA data recorded using the SC sensors are categorized as non-stationery signals [**?**], [**?**]. Hence, multiresolution analysis techniques are essentially suitable to study the qualitative components of these kinds of bio-signals [**?**]. Note that continuous wavelet transform (CWT) is one of the strongest and most widely used analytical tools for multiresolution analysis. CWT has received considerable attention in processing signals with non-stationary spectra [**?**], [**?**]; therefore, it is utilized here to perform the time-frequency analysis of the EDA signals. In contrast to many existing methods that utilize the wavelet coefficients of the raw signal to extract features, our proposed method is essentially based on the spectrogram of the original data in a specific range of frequency (0.5, 50)Hz, which provides more information for other post-processing steps (i.e., feature extraction and classification). We apply the wavelet transform at various scales corresponding to the aforementioned frequency range to calculate the spectrogram of the raw signal (i.e., Short Time Fourier Transform (STFT), can also be used to calculate the spectrogram of the raw signal). In addition, as opposed to many related studies that utilize real-valued wavelet functions for feature extraction purposes, we have employed the complex Morlet (C-Morlet) function with the proposed approach, as it takes into account both the real and imaginary components of the raw signal, leading to a more detailed feature extraction.

The wavelet transform of a 1-D signal provides a decomposition of the time-domain sequence at different scales, which are inversely related to their frequency contents [**?**], [**?**] . This requires the time-domain signal under investigation to be convolved with a time-domain function known as "mother wavelet". The CWT applies the wavelet function at different scales with continuous time-shift of the mother wavelet over the input signal. As a consequence, it helps represent the EDA signals at different levels of resolution. For instance, it results in large coefficients in the transform domain when the wavelet function matches the input signal, providing a multiscale representation of the EDA signal.

Using a finite energy function Ψ(t) concentrated in the time domain, the CWT of a signal x(t) is given by X(α,b) as follows [**?**]:

$$X(a,b) = \int_{-\infty}^{+\infty} x(t) \frac{1}{\sqrt{a}} \Psi(\frac{t-b}{a}) dt$$

where, α, is the scale factor and represents dilation or contraction of the wavelet function and b is the translation parameter that slides this function on the time-domain sequence under analysis. Therefore, Ψ(α,b) is the scaled and translated version of the corresponding mother wavelet. "*" is the conjugation operator.

Note that the wavelet coefficients obtained from Eq. (1) essentially evaluate the correlation between the signal x(t) and the wavelet function used at different translations and scales. This implies that the wavelet coefficients calculated over a range of scales and translations can be combined to reconstruct the original signal as follows:

$$x(t) = \int_{-\infty}^{+\infty} \int_{-\infty}^{+\infty} X(a,b) \Psi(\frac{t-b}{a}) da db$$

4.2.2 Wavelet-Based Feature Extraction and SVM

It has been shown that the wavelet-domain feature space can improve the recognition performance of different human activities using the signals emanated from the body responses [**?**]. Therefore, it essentially enhances the classification performance due to the more distinctive feature space provided.

In this paper, we focus on the time-frequency analysis of the EDA signal to provide a new feature space based on which an emotion classification task can be done. Figure 1 shows the amplitude of the CWT of a sample EDA signal at different scales using a complex Morlet (C-Morlet) wavelet function. Different scales of the wavelet functions are convolved with the original EDA signal to highlight different features of the raw data. As can be seen inside the bottom box, when the scaling parameter of the wavelet function increases, the larger features of the input signal are augmented. As can be seen, due to the localization property of the CWT, different structures of the input signal are extracted at each level of decomposition, providing useful information for analyzing the recorded EDA signals.

In this work, we have employed the C-Morlet wavelet function to process the acquired EDA signals, as it has been well used for time-frequency analysis of different bio-signals and classification [**?**]. Figure 2 shows the wavelet-based feature extraction, Using the C-Morlet mother wavelet, the real and imaginary wavelet coefficients are calculated at different scales. Then, the amplitude of these coefficients is calculated to provide the corresponding spectrogram. This spectrogram is then used as the feature space.

On the other hand, the detailed structures of the signal are better extracted when the scaling factor decreases.. Note

that the impact of different families of the wavelet functions (e.g., Symlets, Daubechies, Coiflets) on the emotion classification will be evaluated in the next subsection. The equation of the C-Morlet mother wavelet with fc as its central frequency and fb as the bandwidth parameter is given as follows:

$$\Psi(t) = \frac{\exp(-t^2/f_b)}{\sqrt{(\pi f_b)}} \exp(j2\pi f_c t)$$

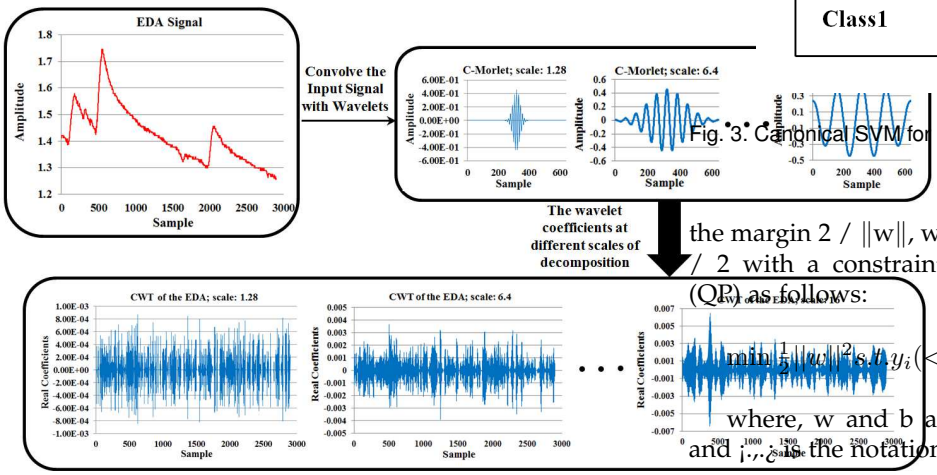

Fig. 1. The CWT of a typical EDA signal using the C-Morlet mother wavelet.

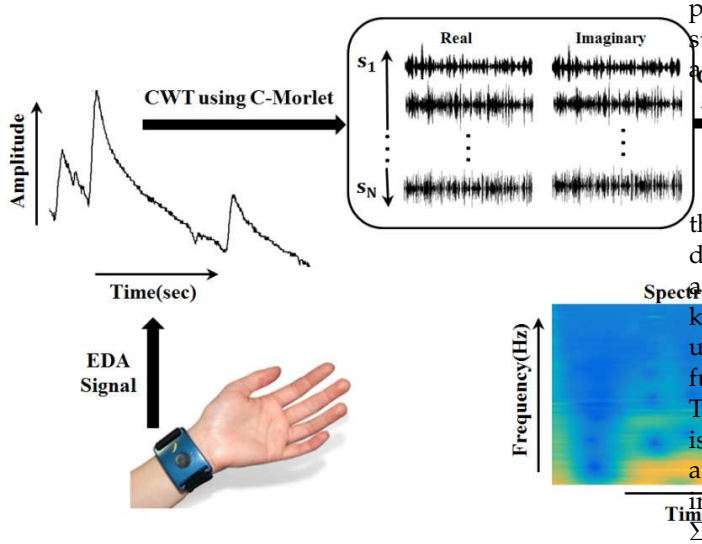

Fig. 2. The wavelet-based feature extraction.

The SVM classifier tends to separate data $D = \{x_i, y_i\}_{i=1}^N, x_i \in^d, y_i \in \{-1, +1\}$ by drawing an optimal hyperplane ¡w,x¿+b=0 between classes such that the margin between them becomes maximum [?]. With reference to Figure 3, The decision boundary is shown by OH. Two hyperplanes H1 and H2 pass the support vectors that are circled inside the figure. H1 and H2 are the supporting planes and the optimal hyperplane (OH) splits this margin such that it stands at the same distance from each supporting hyperplane. This implies that the margin between H1 and H2 is equal to 2 / ‖w‖. In terms of linearly separable classes, the classifier is obtained by maximizing

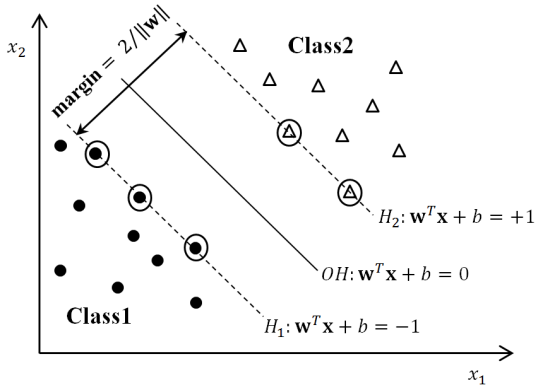

Fig. 3. Canonical SVM for classifying two linearly separable classes.

the margin 2 / ‖w‖, which is equivalent to minimizing ‖w‖ / 2 with a constraint in convex quadratic programming (QP) as follows:

$$\min \frac{1}{2}||w||^2 s.t. y_i(< w, x_i > +b) \geq 1$$

where, w and b are the parameters of the hyperplane and ¡.,.¿ is the notation of the inner product.

However, different classes are seldom separable by a hyperplane since their samples are overlapped in the feature space. In such cases, a slack variable $\xi_i \geq 0$ and a penalty parameter C ≥ 0 are used with the optimization step to obtain the best feasible decision boundary. It is given as:

$$\min \frac{1}{2}||w||^2 + C(\Sigma_{i=1}^N \xi_i) s.t. y_i(< w, x_i > +b) \geq 1 - \xi_i$$

Usually, various kernel functions are used to deal with the nonlinearly separable data. As a result, the original data xi is mapped onto another feature space through a projection function $\varphi(\cdot)$. It is not necessary to exactly know the equation of the projection $\varphi(\cdot)$, but one can use a kernel function $k(x_i, x_j) =< \varphi(x_i), \varphi(x_j) >$. This function is symmetric and satisfies the Mercer's conditions. The Mercer's conditions determine if a candidate kernel is actually an inner-product kernel. Let $k(x_i, x_j)$ be a continuous symmetric kernel defined in the closed interval $t_1 \leq t \leq t_2$, the kernel can be expanded into series $\Sigma(n = 1)^\infty = \lambda_n \varphi_n(x_i)\varphi_n(x_j)$, where $\lambda_n > 0$ are called eigenvalues and functions φn are called eigenvectors in the expansion. The fact that all the eigenvalues are nonnegative means that the kernel is positive semidefinite [?].

To maximize the margin, H1 and H2 are pushed apart until they reach the support vectors on which the solution depends. To solve this optimization problem, the Lagrangian dual of Eq. (5) is used as follows:

$$\max_\alpha \Sigma_{i=1}^N \alpha_i - \frac{1}{2}\Sigma_{i=1}^N \Sigma_{j=1}^N y_i y_j \alpha_i \alpha_j k(x_i, x_j)$$
$$s.t. 0 \leq \alpha_i \leq C, \Sigma_{i=1}^N \alpha_i y_i = 0, i = 1, ..., N$$

where, α_is are the Lagrangian multipliers in which just a few number of them are non-zero. These non-zero values

are corresponding to the support vectors determining the parameters of the hyperplane $w = \Sigma_(i = 1)^N \alpha_i y_i x_i$. Therefore, the label of the test sample (y_z) is given by:

$$y_z = sgn(\Sigma_{i=1}^{N} \alpha_i y_i k(x_i, z)) + b$$

5 Experiment Results

6 Conclusion

The conclusion goes here.

Appendix A
Proof of the First Zonklar Equation

Appendix one text goes here.

Appendix B

Appendix two text goes here.

Acknowledgments

The authors would like to thank...

References

[1] H. Kopka and P. W. Daly, *A Guide to LaTeX*, 3rd ed. Harlow, England: Addison-Wesley, 1999.

PLACE PHOTO HERE

Michael Shell Biography text here.

John Doe Biography text here.

Jane Doe Biography text here.